Biomedical Science and Engineering, 2015, Vol. 3, No. 2, 35-40
Available online at http://pubs.sciepub.com/bse/3/2/2

DOI:10.12691/bse-3-2-2

Challenges and Advances in Near Infrared Spectroscopy for Evaluating Hemodynamics in Brain

Yasutomo Nomura*

Department of Systems Life Engineering, Maebashi Institute of Technology, Kamisadori, Maebashi, Japan
*Corresponding author: ynomura@maebashi-it.ac.jp

Received August 27, 2015; Revised September 27, 2015; Accepted October 09, 2015

Abstract Near infrared spectroscopy is a powerful technique to evaluate hemodynamics in cerebral tissue where the light used is subject to the low scattering effect. In this wavelength range, hemoglobin has the characteristic absorption spectra. Because of the noninvasive method, this gives valuable information containing venous blood to the clinical field such as cardiac surgery, neurosurgery and pediatrics. Although the technique originates from classical biochemistry with clear solution, researchers have proposed creative ideas to be suitable for measuring hemodynamics in living tissue optically. In this mini-review, theoretical basis from Lambert-Beer law to multiwavelength method and derivation of the linear relationship between absorption and concentration of pigments from the time-resolved method are described. Furthermore the recent advances are also outlined.

Keywords: *ear infrared spectroscopy, hemoglobin, absorption, concentration, Lambert-Beer law, time resolved spectroscopy*

Cite This Article: Yasutomo Nomura, "Challenges and Advances in Near Infrared Spectroscopy for Evaluating Hemodynamics in Brain." *Biomedical Science and Engineering*, vol. 3, no. 2 (2015): 35-40. doi: 10.12691/bse-3-2-2.

1. Introduction

When the light is applied to a living tissue, it is subject to reflection, scattering, and absorption as shown in Figure 1 [1]. Reflectance occurs in the tissue surface, which is dependent on an incident angle to the surface. The light within the tissue undergoes scattering and absorption that are dependent on the wavelengths. Some of the light can be detected as diffuse reflectance or diffuse transmittance.

Scattering increases when the wavelengths become short [2]. Since the wavelengths of light in near infrared region are longer than that of visible region, the scattering effect is considered to be weak. On the other hand, absorption occurs in specific wavelengths which are determined by spectral properties of biomolecules within the tissue. Water within the tissue absorbs the light above 1300 nm strongly [3]. From the viewpoints of scattering and absorption, therefore, the near infrared light ranged from 700 to 1300 nm (NIR) is considered to be proper for noninvasively spectroscopic measurement in the living tissue.

Furthermore, hemoglobin in red blood cells has favorable characteristics in NIR, e.g., the absorption is dependent on the oxygenation state [4]. Therefore, using NIR, it may be possible to evaluate hemodynamics such as changes in blood volume and hemoglobin oxygenation state. Especially, the noninvasive measurement of the hemodynamics in cerebral tissue draws the attention of both clinical and research fields. In this mini-review, challenges and recent advances on tissue optics for evaluating hemodynamics are discussed.

2. Cerebral Tissue Spectra and Its Components in NIR

In NIR, major components with strong absorption were hemoglobin, cytochrome oxidase, water and fat [3,4,5,6]. Absorption spectra of hemoglobin of 100 % oxygenated form differed from that of 0% largely [4]. In this wavelength range, 805 nm was an isosbestic point for oxygenation and deoxygenation of hemoglobin. When the wavelengths were shorter than 805 nm, absorption of deoxyhemoglobin was stronger than that of oxyhemoglobin and an absorption peak appeared at 760 nm. In contrast, when the wavelengths were longer than 805 nm, oxyhemoglobin absorbed the light stronger than deoxyhemoglobin.

Cytochrome oxidase is the terminal member of mitochondrial respiratory chain. This contains copper and is heme-protein like hemoglobin. When the enzyme was oxidized, a weak absorption band existed in the 780 – 870 nm region in which there was a broad maximum from 820 to 840 nm [6]. Upon reduction of the enzyme, this band disappeared. Water of first principal components within a living tissue absorbed the light [3]. The longer the wavelengths became up to 2500 nm, the stronger water absorbed the light. It had 4 absorption peaks of 970, 1190, 1450, 1940 nm. Fat had an absorption peak at 930 nm [5]. Although the glucose absorption spectrum had almost no characteristic feature in NIR, there was the overtone band

between 1530 and 1820 nm [7]. In the wavelengths range between 700 and 780 nm, hemoglobin alone would show spectral changes which is dependent on oxygen concentration in the tissue.

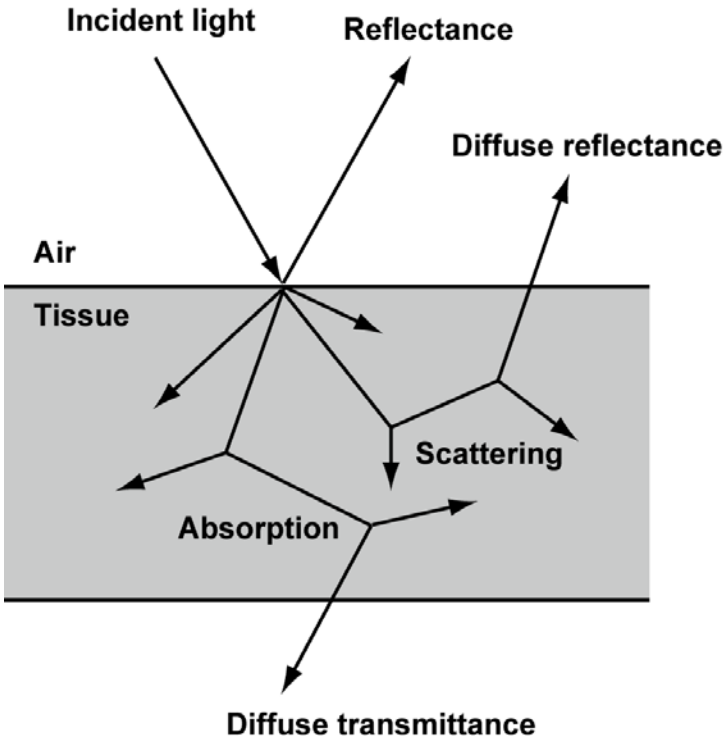

Figure 1. Several behaviors of light in an irradiated tissue

3. Lambert-Beer Law

In NIR spectroscopy, many researchers and physicians used the method expanded from Lambert-Beer law that stands for dilute and transparent solutions [4]. When monochromatic light transmits homogeneous and transparent media containing some pigments such as hemoglobin, the light intensity decreases due to absorption by pigments. In Lambert law, the ratio of decreases in light through solution containing pigments *dI* against the intensity of incident light *I* is proportional to thickness of the solution *dx*, as shown in Figure 2A.

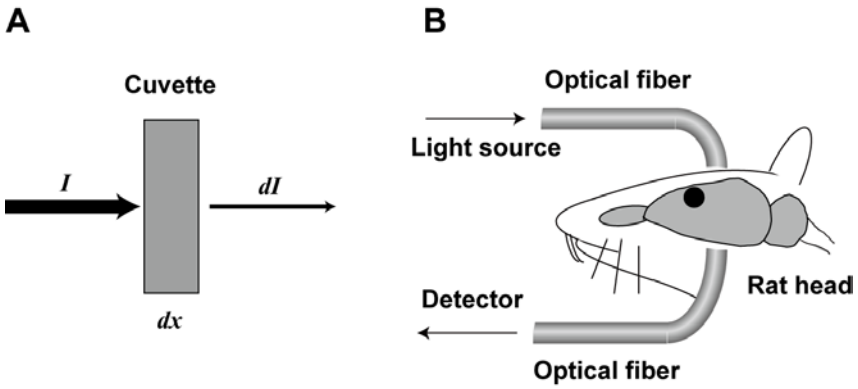

Figure 2. Block diagram of absorbance measurement. See text. A: Light intensity through the pigment solution in a cuvette, *I*, decreases with the thickness *dx* in Lambert law. B: Concentration changes in hemoglobin of rat brain were measured through optical fibers. As a light source, a halogen lamp of continuous illumination or a picosecond pulsed laser was used

$$\frac{dI}{I} = -\alpha dx,$$

where α is a proportional constant. When the intensity at $x = 0$ is replaced as I_0, we can write

$$\ln \frac{I_0}{I} = \alpha x .$$

Since we usually use common logarithm in tissue optics, new constant k is replaced to $\log e \cdot \alpha$

$$\log \frac{I_0}{I} = kx.$$

The left term of common logarithm represents absorbance A which is proportional to the optical pathlength x.

Furthermore, when the number of pigments in unit area of luminous flux is s, the number of pigments in luminous flux, n, increases with x. Here we can write $n = sx$. Concentration of pigments C is proportional to n and the constant is used as t.

$$A = \beta C,$$

where $\beta = k / st$. Absorbance is proportional to C, which is Beer law. In Lambert-Beer law, absorbance is proportional to both of concentration C and optical pathlength x.

$$A = \varepsilon C x, \quad (1)$$

where ε is molar absorption coefficient of pigment.

4. Principle of NIR Spectroscopy

Pulse oximetry employed the visible light as well as NIR and was often used for evaluation of oxygen saturation in arterial blood. It measured an increase in the light absorption due to the systolic increase in arterial blood volume, which provided information on respiratory function [8]. In contrast, data in NIR spectroscopy contained information on hemodynamics in venous blood or oxygen consumption in the tissue [4]. This mini-review focuses on NIR spectroscopy.

The assumption in NIR spectroscopy was the linear dependence of the changes in absorbance at a certain wavelength on oxy- or deoxyhemoglobin concentration in a brain [4]. However, light-scattering system like a living tissue is different from clear solution in which Lambert-Beer law stands. Therefore, although such a linear relationship cannot be strictly extended to NIR spectroscopy, it has often been used as an approximation within a narrow concentration range that could occur under physiological conditions. Before discussion about the linearity, procedures required for NIR spectroscopy is outlined. As shown in Figure 2B, diffuse transmittance of a brain through optical fiber system has been detected generally with a continuous illumination.

At wavelength λ_1, where the absorbance change of a tissue ΔA_1 is the summation of that due to concentration changes in oxyhemoglobin $[HbO_2]$ and deoxyhemoglobin $[Hb]$, according to the Beer law,

$$\Delta A_1 = k_1 \Delta[HbO_2] + k_1' \Delta[Hb], \quad (2)$$

where k_1 and k_1' are the absorption coefficients for oxy- and deoxyhemoglobin, respectively. These values may be different from the molar absorption coefficients obtained in transparent solutions because of the scattering effect and the high localization of hemoglobin in red blood cells under *in situ* conditions. The absorbance change at another wavelength λ_2 can be written as

$$\Delta A_2 = k_2 \Delta[HbO_2] + k_2' \Delta[Hb]. \quad (3)$$

From *Eqs.*2 and 3, the change of oxyhemoglobin concentration in a tissue can be written as

$$\Delta[HbO_2] = K_1 [\Delta A_1 - (k_1'/k_2')\Delta A_2], \quad (4)$$

where $K_1 = k_2'/(k_1 k_2' - k_1' k_2)$. Because K_1 is a proportional constant, $\Delta[HbO_2]$ is linearly related to $\Delta A_1 - (k_1'/k_2')\Delta A_2$. Similarly the change in total hemoglobin concentration within a tissue is expressed by

$$\Delta[HbO_2] + \Delta[Hb] = K_2 \left(\Delta A_1 - \frac{(k_1' - k_1)}{(k_2' - k_2)} \Delta A_2 \right), \quad (5)$$

where $K_2 = (k_2' - k_2)/(k_1 k_2' - k_1' k_2)$. Because the changes in oxidation of cytochrome oxidase caused almost no absorbance change in the wavelengths which were shorter than 780 nm of NIR, the authors chose $\lambda_1 = 700$ and $\lambda_2 = 730$ nm to monitor the oxygenation state and the concentration of hemoglobin. When the NIR spectroscopy was applied to living tissue, the absorption coefficients required to be determined experimentally because the value would be different from that of clear solution.

First, k_{700}'/k_{730}' in *Eq.* 4 should be determined *in situ* in order to measure the oxyhemoglobin concentration in a tissue. In the study, the authors asphyxiated the rats and the external jugular veins were cut bilaterally. These conditions assured that the brain contained deoxyhemoglobin alone. Then, when oxygen free saline was infused repeatedly into the left carotid artery, a decrease in deoxyhemoglobin resulted in both changes in ΔA_{700} and ΔA_{730} as shown in Figure 3A. Because the brain contains no oxyhemoglobin, *Eq.*4 can be written as $\Delta A_{700} = (k_{700}'/k_{730}')\Delta A_{730}$. When the relationship between ΔA_{700} and ΔA_{730} obtained from the animal experiment was plotted, the slope was $k_{700}'/k_{730}' = 1.20$ (Figure 3B).

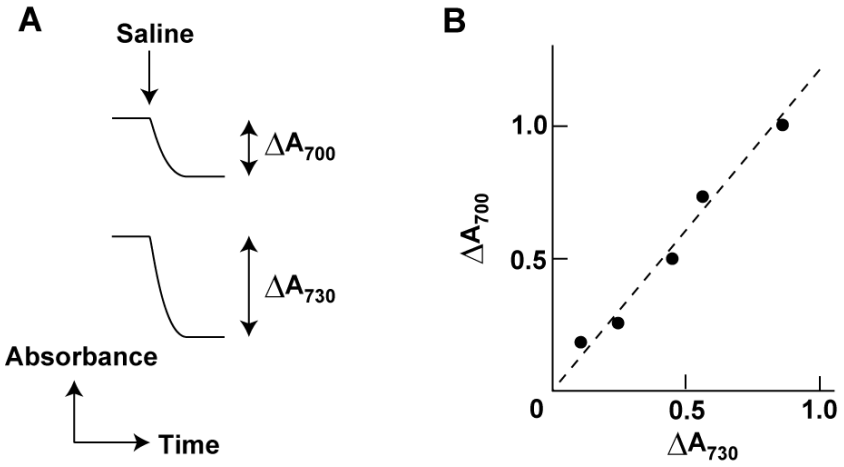

Figure 3. Scheme of deoxyhemoglobin dilution experiments in an asphyxiated rat. A: Absorbance decreased in response to the infusion of saline into the brain through a carotid artery. The repeated infusion resulted in changes in absorbance at 700 and 730 nm. B: Summary of the absorbance changes

Secondary, they determined the value of $(k_{700}'-k_{700})/(k_{730}'-k_{730})$ in *Eq.* 5 from data of the rat experiment to calculate the total hemoglobin concentration. When oxygen in the inspired gas was decreased stepwise from 95% to 7.5% under hypercapnic conditions (+5% CO_2), the total hemoglobin concentration in the brain kept unchanged. Because the right term of Eq.5 is equal to 0, $\Delta A_{700}=(k_{700}'-k_{700})/(k_{730}'-k_{730})\Delta A_{730}$. Under the conditions, the decreases in oxyhemoglobin concentration and the increases in deoxyhemoglobin caused changes in both ΔA_{700} and ΔA_{730} as similar with Figure 3. When the relationship between ΔA_{700} and ΔA_{730} obtained experimentally was plotted, the slope was $(k_{700}'-k_{700})/(k_{730}'-k_{730})=1.52$.

Finally, since hemoglobin in the rat brain is known to be mostly in the oxygenated form under hypercapnic and hyperoxic conditions (95% O_2 +5% CO_2), $\Delta[Hb]=0$ in spite of saline infusion with small amount. From *Eq.*4 and *Eq.*5, $K_1/K_2=(\Delta A_{700}-1.52\Delta A_{730})/(\Delta A_{700}-1.20\Delta A_{730})$. When the rapid injections of 0.25 ml saline caused the decrease in oxyhemoglobin as shown in Figure 4A, the change in oxyhemoglobin concentration for $\Delta A_{700}-1.20\Delta A_{730}$ in *Eq.*4 and for $\Delta A_{700}-1.52\Delta A_{730}$ in *Eq.*5 can be calculated using ΔA_{700} and ΔA_{730} obtained experimentally. In the same way, the rapid injection of 0.5 ml saline resulted in more dilution of oxyhemoglobin in the brain. Thus the ratio of $\Delta A_{700}-1.52\Delta A_{730}$ to $\Delta A_{700}-1.20\Delta A_{730}$ was $2.1=K_1/K_2=k_{730}'/\begin{pmatrix}k_{730}'\\-k_{730}\end{pmatrix}$ in both cases of 0.25 and 0.5 ml injection (Figure 4B).

From these three equations, $k_{700}'/k_{730}'=1.20$, $\begin{pmatrix}k_{700}'\\-k_{700}\end{pmatrix}/\begin{pmatrix}k_{730}'\\-k_{730}\end{pmatrix}=1.52$, $k_{730}'/\begin{pmatrix}k_{730}'\\-k_{730}\end{pmatrix}=2.1$, the relative values for *in situ* absorption coefficients $k_{700}, k_{730}, k_{700}', k_{730}'$ can be calculated to be 1.0, 1.1, 2.5 and 2.1, respectively. Using these values, it is possible to evaluate relative oxygenation state in a living tissue. These values were different from corresponding values for a clear hemoglobin solution. In NIR spectroscopy, hemodynamics such as changes in total hemoglobin and oxyhemoglobin was obtained by the use of *in situ* absorption coefficients.

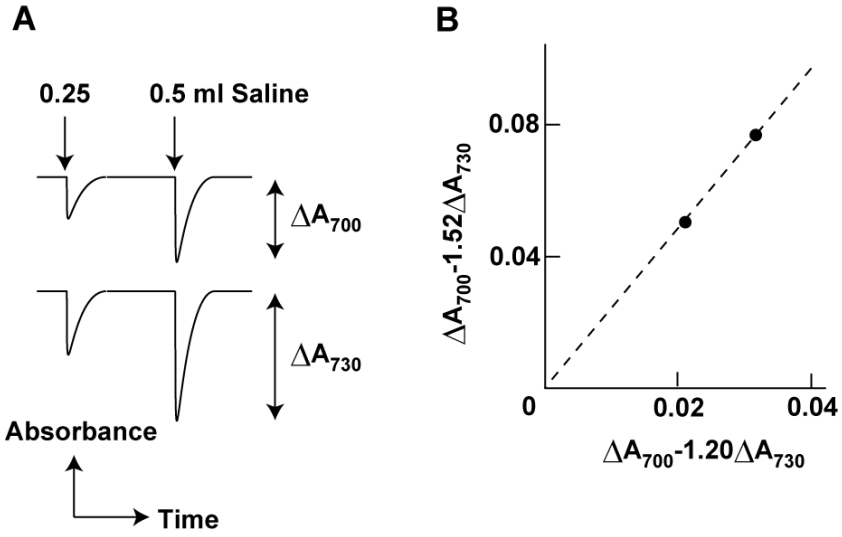

Figure 4. Scheme of oxyhemoglobin dilution experiments under hypercapnic and hyperoxic conditions. Absorbance decreased transiently in response to the infusion of saline into the brain through a carotid artery. B: Summary of K_1 and K_2 in *Eq.* 4 and 5 by calculating the absorbance changes

5. Time-resolved Method

Although NIR spectroscopy relied on the linear relationship between absorbance change and hemoglobin concentration as described above, several investigators pointed out that the optical pathlength through scattering media such as living tissues was a function of absorption [9,10]. Therefore, optical pathlength which would be longer than the distance between optodes on the tissue surface due to scattering may vary with changes in hemoglobin oxygenation state. This concept that seemed to be difficult to measure hemodynamics quantitatively was widely accepted, which delayed the clinical use of NIR spectroscopy.

Although it was difficult to measure optical pathlength directly using continuous illumination, time resolved method with pulsed laser permitted to trace each optical pathlength of the detected photons (Figure 2B). By the use of the method, it was proposed that the intensity of photons propagating along a nonlinear path through a scattering medium was exponentially attenuated by absorption [11,12,13]. This suggested that the attenuation of incident light by absorption was independent of scattering. Using this time-resolved method, an empirical linear relationship in NIR spectroscopy was derived [14].

In the time resolved analysis with picosecond pulse laser as shown in Figure 5, the Lambert-Beer law with optical pathlength x is temporally resolved and absorbance at a certain time t, $A(t)$, can be expressed as follows:

$$A(t)=\log[I_0(t)/I(t)]=\varepsilon Cvt \qquad (6)$$

where $I_0(t)$ is the intensity of light as a function of time taken by photons to pass through the scattering medium

without any pigments. $I(t)$ is that with pigments. ε, C, and v represent the molar absorption coefficient and concentration of pigments and light velocity in water, respectively. Time zero was defined as the time when the peak intensity of the light that had pulse width of ~ 40 picoseconds reached the illuminated surface.

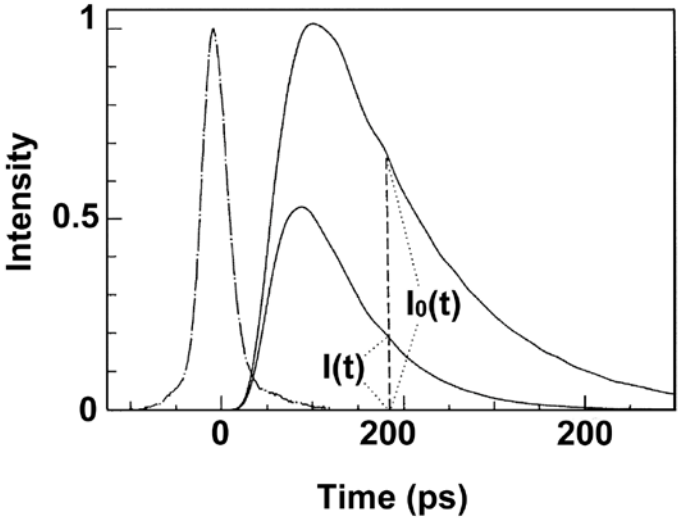

Figure 5. Time resolved analysis of pulsed light though an irradiated tissue. Dashed dotted line denotes pulsed light entering scattering medium such as a living tissue. Solid lines show intensity profiles of the light detected from the scattering medium with and without pigments, $I(t)$ and $I_0(t)$, respectively

In the both model of homogeneous phantom at 1064 nm and the Monte Carlo simulation, there was the linear relationship between the observed values of $A(t)$ and t at various hemoglobin concentrations within the temporal range of adequate intensity of $I(t)$, which is expected in *Eq*.6 [12,15]. Absorbance per time of picosecond was proportional to both hemoglobin concentration C and absorption coefficient ε. The value of ε obtained experimentally agreed with that of the clear solution. Furthermore, when transmittance in the rat brain was examined using time-resolved Lambert-Beer law of *Eq*.6, the absolute concentration and the oxygen saturation of hemoglobin were consistent with expected values. The temporal profile of rat brain was reproduced by Monte Carlo simulation using absorption and scattering coefficients of rat brain [14].

When the temporal profiles of rat brain under different oxygenation states were integrated over time, the absorbance difference was linearly related to the changes in the absorption coefficient. When the simulated profiles were integrated temporally, there was a linear relationship within the absorption coefficient which was predicted for fractional inspiratory oxygen concentration from 10 to 100%. In the case beyond the range of the absorption coefficient, the deviation from linearity was slight.

When the linear relationship is derived from *Eq*. 6 by temporal integration, absorbance can be written as

$$A(\mu) = \log e \ln\left[\frac{\int I_0(t)\,dt}{\int I_0(t)\exp(-\mu v t)\,dt}\right] \qquad (7)$$

where $\mu = \varepsilon C / \log e$. When the absorption coefficient at a normal state, for example 20% FiO2, is μ_{an} and the changing absorption coefficient within the physiological range, for example, from fractional inspiratory oxygen concentration 100% to 10%, is μ_{ap}, the difference between μ_{an} and μ_{ap} is consider to be much smaller than μ_{an}. Under this condition, *Eq*. 7 can be approximated to the first-order term of the Taylor series:

$$\begin{aligned} A(\mu_{ap}) &= A(\mu_{an}) + \frac{dA}{d\mu}(\mu_{an})(\mu_{ap} - \mu_{an}) \\ &= \left(\log e \cdot \frac{v\int t I_0(t)\exp(-\mu_{an} v t)\,dt}{\int I_0(t)\exp(-\mu_{an} v t)\,dt}\right)\mu_{ap} \\ &\quad + \text{constant} \end{aligned} \qquad (8)$$

where

$$\text{constant} = A(\mu_{an}) - \left(\log e \cdot \frac{v\int t I_0(t)\exp(-\mu_{an} v t)\,dt}{\int I_0(t)\exp(-\mu_{an} v t)\,dt}\right)\mu_{an}.$$

Eq. 8 is a linear function of $\mu_{ap} \cdot \log e (= \varepsilon C)$ and represents the linear relationship expected previously between the absorbance and absorption coefficients in NIR spectroscopy. The factor of proportion is expressed as D_{scatt}:

$$D_{scatt} = \frac{v\int t I_0(t)\exp(-\mu_{an} v t)\,dt}{\int I_0(t)\exp(-\mu_{an} v t)\,dt}$$

D_{scatt} expresses an optical pathlength using temporal integration of intensity profile of pulsed light through living tissue, which cannot be measured by continuous illumination. In this case, a specific time taken until the detection of light entering tissue should not be an arithmetic mean of detecting time but a weighted average by weighting and averaging detecting time according to the intensity. A product of the specific time and light velocity in water would be optical pathlength through the tissue D_{scatt} which is independent of changes in absorption coefficient within physiological range.

Therefore, the linear relationship between absorbance difference and changes in absorption coefficient within

physiological range would be an appropriate assumption in NIR spectroscopy.

6. Perspective

Recently, the devices of NIR spectroscopy have become smaller and has been improved as for user interfaces and calibration procedures. Then, the importance of NIR spectroscopy grows as a monitoring tool for broad clinical use. For example, it was used to assess cerebral autoregulation [16] and to choose anesthetic [17]. Researchers pay attention to the selective quantitative measurement of cerebral hemoglobin during brain activation together with functional magnetic resonance imaging data analysis. The near-infrared optical tomography was reported also [18]. Furthermore, researchers used it for a noninvasive functional imaging and reported the evaluation of working memory performance [19]. When the neural activity-dependent optical signal was analyzed carefully, changes in hemodynamics as well as that in cell swelling were observed [20,21]. Laser doppler flowmetry with NIR was also used to measure blood flow [22]. Changes in cerebral blood flow which was correlated with neural activity were monitored by dynamic light scattering [23]. In addition, it may be possible to monitor the electrical activity of animal brain optically because clear images of intracranial quantum dots in NIR were obtained [24] and optical properties of quantum dots were dependent on the cell membrane potential [25]. Therefore, the importance of NIR would grow as an optical window in medical field.

Acknowledgements

This work was financially supported in part by JSPS KAKENHI Grant Number 23500523, Grant-in-Aid for Scientific Research (C) from Japan Society for the Promotion of Science (JSPS).

References

[1] F. F. Jobsis, "Noninvasive, infrared monitoring of cerebral and myocardial oxygen sufficiency and circulatory parameters," Science, vol. 198, pp. 1264-7, Dec 23 1977.

[2] H. J. van Staveren, C. J. M. Moes, J. van Marie, S. A. Prahl, and M. J. C. van Gemert, "Light scattering in Intralipid 10% in the wavelength range of 400-1100 nm," Appl Opt, vol. 30, pp. 4507-4514, 1991.

[3] H. Büning-Pfaue, "Analysis of water in food by near infrared spectroscopy," Food Chem, vol. 82, pp. 107-115, 7// 2003.

[4] O. Hazeki and M. Tamura, "Quantitative analysis of hemoglobin oxygenation state of rat brain in situ by near-infrared spectrophotometry," J Appl Physiol (1985), vol. 64, pp. 796-802, Feb 1988.

[5] J. M. Conway, K. H. Norris, and C. E. Bodwell, "A new approach for the estimation of body composition: infrared interactance," Am J Clin Nutr, vol. 40, pp. 1123-30, Dec 1984.

[6] Y. Hoshi, O. Hazeki, Y. Kakihana, and M. Tamura, "Redox behavior of cytochrome oxidase in the rat brain measured by near-infrared spectroscopy," J Appl Physiol (1985), vol. 83, pp. 1842-8, Dec 1997.

[7] P. Du Yi, Y. Z. Liang, S. Kasemsumran, K. Maruo, and Y. Ozaki, "Removal of interference signals due to water from in vivo near-infrared (NIR) spectra of blood glucose by region orthogonal signal correction (ROSC)," Anal Sci, vol. 20, pp. 1339-45, Sep 2004.

[8] M. Nitzan, A. Romem, and R. Koppel, "Pulse oximetry: fundamentals and technology update," Med Devices (Auckl), vol. 7, pp. 231-9, 2014.

[9] D. A. Benaron, C. D. Kurth, J. M. Steven, M. Delivoria-Papadopoulos, and B. Chance, "Transcranial optical path length in infants by near-infrared phase-shift spectroscopy," J Clin Monit, vol. 11, pp. 109-17, Mar 1995.

[10] S. T. Flock, M. S. Patterson, B. C. Wilson, and D. R. Wyman, "Monte Carlo modeling of light propagation in highly scattering tissue--I: Model predictions and comparison with diffusion theory," IEEE Trans Biomed Eng, vol. 36, pp. 1162-8, Dec 1989.

[11] Y. Nomura, O. Hazeki, and M. Tamura, "Exponential attenuation of light along nonlinear path through the biological model," Adv Exp Med Biol, vol. 248, pp. 77-80, 1989.

[12] Y. Nomura and M. Tamura, "Quantitative analysis of the hemoglobin oxygenation state of rat brain in vivo by picosecond time-resolved spectrophotometry," J Biochem, vol. 109, pp. 455-61, Mar 1991.

[13] Y. Nomura and M. Tamura, "Picosecond time of flight measurement of living tissue: time resolved Beer-Lambert law," Adv Exp Med Biol, vol. 316, pp. 131-6, 1992.

[14] Y. Nomura, O. Hazeki, and M. Tamura, "Relationship between time-resolved and non-time-resolved Beer-Lambert law in turbid media," Phys Med Biol, vol. 42, pp. 1009-22, Jun 1997.

[15] Y. Hasegawa, Y. Yamada, M. Tamura, and Y. Nomura, "Monte Carlo simulation of light transmission through living tissues," Appl Opt, vol. 30, pp. 4515-20, Nov 1 1991.

[16] K. Brady, B. Joshi, C. Zweifel, P. Smielewski, M. Czosnyka, R. B. Easley, et al., "Real-time continuous monitoring of cerebral blood flow autoregulation using near-infrared spectroscopy in patients undergoing cardiopulmonary bypass," Stroke, vol. 41, pp. 1951-6, Sep 2010.

[17] J. Schoen, L. Husemann, C. Tiemeyer, A. Lueloh, B. Sedemund-Adib, K. U. Berger, et al., "Cognitive function after sevoflurane- vs propofol-based anaesthesia for on-pump cardiac surgery: a randomized controlled trial," Br J Anaesth, vol. 106, pp. 840-50, Jun 2011.

[18] Y. Hoshi, "Towards the next generation of near-infrared spectroscopy," Philos Trans A Math Phys Eng Sci, vol. 369, pp. 4425-39, Nov 28 2011.

[19] Y. Ogawa, K. Kotani, and Y. Jimbo, "Relationship between working memory performance and neural activation measured using near-infrared spectroscopy," Brain Behav, vol. 4, pp. 544-51, Jul 2014.

[20] M. Nemoto, Y. Nomura, C. Sato, M. Tamura, K. Houkin, I. Koyanagi, et al., "Analysis of optical signals evoked by peripheral nerve stimulation in rat somatosensory cortex: dynamic changes in hemoglobin concentration and oxygenation," J Cereb Blood Flow Metab, vol. 19, pp. 246-59, Mar 1999.

[21] Y. Nomura, F. Fujii, C. Sato, M. Nemoto, and M. Tamura, "Exchange transfusion with fluorocarbon for studying synaptically evoked optical signal in rat cortex," Brain Res Brain Res Protoc, vol. 5, pp. 10-5, Feb 2000.

[22] A. N. Obeid, G. Dougherty, and S. Pettinger, "In vivo comparison of a twin wavelength laser Doppler flowmeter using He-Ne and laser diode sources," J Med Eng Technol, vol. 14, pp. 102-10, May-Jun 1990.

[23] J. Lee, H. Radhakrishnan, W. Wu, A. Daneshmand, M. Climov, C. Ayata, et al., "Quantitative imaging of cerebral blood flow velocity and intracellular motility using dynamic light scattering-optical coherence tomography," J Cereb Blood Flow Metab, vol. 33, pp. 819-825, 06//print 2013.

[24] Y. Tsukasaki, M. Morimatsu, G. Nishimura, T. Sakata, H. Yasuda, A. Komatsuzaki, et al., "Synthesis and optical properties of emission-tunable PbS/CdS core-shell quantum dots for in vivo fluorescence imaging in the second near-infrared window," RSC Advances, vol. 4, pp. 41164-41171, 2014.

[25] K. Lugo, X. Miao, F. Rieke, and L. Y. Lin, "Remote switching of cellular activity and cell signaling using light in conjunction with quantum dots," Biomed Opt Express, vol. 3, pp. 447-54, Mar 1 2012.